2009

Oxygen-mediated enhancement of primary hepatocyte metabolism, functional polarization, gene expression, and drug clearance

Srivatsan Kidambi
University of Nebraska-Lincoln, skidambi2@unl.edu

Rubin S. Yarmush
Harvard Medical School

Eric Novik
HμREL Corporation, Beverly Hills, CA

Piyun CHao
HμREL Corporation, Beverly Hills, CA

Martin L. Yarmush
Harvard Medical School

See next page for additional authors

Oxygen-mediated enhancement of primary hepatocyte metabolism, functional polarization, gene expression, and drug clearance

Srivatsan Kidambi[a], Rubin S. Yarmush[a], Eric Novik[b], Piyun Chao[b], Martin L. Yarmush[a], and Yaakov Nahmias[a,c,1]

[a]Center for Engineering in Medicine, Massachusetts General Hospital, Harvard Medical School, Boston, MA 02111; [b]HμREL Corporation, Beverly Hills, CA 90211; and [c]The Selim and Rachel Benin School of Computer Science and Engineering, The Hebrew University of Jerusalem, Jerusalem 91904, Israel

Edited by Robert Langer, Massachusetts Institute of Technology, Cambridge, MA, and approved July 23, 2009 (received for review June 20, 2009)

The liver is a major site for the metabolism of xenobiotic compounds due to its abundant level of phase I/II metabolic enzymes. With the cost of drug development escalating to over $400 million/drug there is an urgent need for the development of rigorous models of hepatic metabolism for preclinical screening of drug clearance and hepatotoxicity. Here, we present a microenvironment in which primary human and rat hepatocytes maintain a high level of metabolic competence without a long adaptation period. We demonstrate that co-cultures of hepatocytes and endothelial cells in serum-free media seeded under 95% oxygen maintain functional apical and basal polarity, high levels of cytochrome P450 activity, and gene expression profiles on par with freshly isolated hepatocytes. These oxygenated co-cultures demonstrate a remarkable ability to predict in vivo drug clearance rates of both rapid and slow clearing drugs with an R^2 of 0.92. Moreover, as the metabolic function of oxygenated co-cultures stabilizes overnight, preclinical testing can be carried out days or even weeks before other culture methods, significantly reducing associated labor and cost. These results are readily extendable to other culture configurations including three-dimensional culture, bioreactor studies, as well as microfabricated co-cultures.

drug discovery | liver metabolism | tissue engineering

The liver is the largest internal organ and the hub of carbohydrate, lipid, and protein metabolism. Liver metabolism plays a central role in the clearance, modification, and incidental toxicity of most nutrients and xenobiotics. Consequently drug-induced liver toxicity and unpredicted drug metabolism are major causes of postmarket drug withdrawal (1, 2). With cost of drug development escalating to $400 million/drug there is an urgent need for the development of rigorous models of liver metabolism in the context of ADME/Tox (absorption, distribution, metabolism, excretion, and toxicity) screening. This need is exacerbated by the failure of animal studies to predict drug clearance and toxicity, as well as the disastrous clinical and financial consequences of postmarket drug withdrawal (2, 3).

One model found to be useful in the prediction of drug metabolism is the culture of primary human hepatocytes (4, 5). In current practice, isolated hepatocytes are cultured in suspension, a configuration shown to maintain high levels of cytochrome P450 (CYP450) activity up to 6 h in vitro. This technique allows for the characterization of rapidly clearing drugs (4, 5). However, the inherent difficulties in evaluating the metabolism of slow-clearing drugs under such short time periods bars many promising compounds from clinical validation (4). An alternative approach developed by several groups, including ours, is to support the long-term function of primary hepatocytes using specialized tissue culture configurations (6–8).

Previously, Dunn et al. demonstrated long-term synthetic and metabolic activity in primary hepatocytes entrapped between two layers of collagen (9, 10), while others demonstrated similar enhancement of function in hepatocytes following their aggregation into spheroids (11). An alternative strategy is the coculture of hepatocytes with non-parenchymal cells such as 3T3-J2 fibroblasts or endothelial cells (8, 12, 13). Recently, micropatterns of hepatocytes and 3T3-J2 were shown to acquire high levels of CYP450 gene transcription and metabolic activity following 11 days of culture (14). While these culture configurations offer significant metabolic competence, they do so only after a long adaptation period of between 7 to 10 days of culture during which the primary cells slowly adapt their metabolic activity to the in vitro microenvironment (6, 14).

One strategy to eliminate this long adaptation period and attain a high level of metabolic activity from the onset of culture is to minimize the stress associated with the transition between the in vivo to the in vitro microenvironment. A critical aspect of the microenvironment which is dramatically different between in vivo and in vitro is oxygen supply (15). In vivo a mixture of arterial and venous blood continuously supply over 2,000 nmol/mL of oxygen to hepatocytes, while in vitro oxygen's low solubility in culture media offers less than 200 nmol/mL to the cells (7, 16). While this has traditionally limited hepatocytes to subconfluent cultures (15), oxygen supply becomes an even greater concern during the initial phase of cell attachment when oxygen uptake rates are 300% greater than normal (17, 18). It is not surprising therefore that reducing oxygen concentration negatively affects hepatocyte metabolism (19–21). However, it is surprising that the culture of primary hepatocytes under high partial pressures of oxygen is not reported to improve their metabolic activity (19, 21, 22).

Our recent development of an oxygen-carrying matrix allowed us to identify a negative effect of serum on oxygen-enhanced metabolism (16). As serum has been previously shown to cause loss of hepatocyte polarity and gene expression during the onset of culture (23, 24), it suggests that a serum-free, oxygen-rich microenvironment would minimize adaptation stress and allow for high levels of metabolic activity from the onset of culture. If this hypothesis holds, it suggests a simple approach to enhance the metabolic activity of other highly metabolic cells such as cardiomyocytes, β-cells, or neurons, and could potentially enhance our ability to induce these phenotypes during embryonic stem cell differentiation.

In support of this hypothesis we demonstrate that serum has a predominantly negative effect on the metabolic function of primary rat and human hepatocytes. In the absence of serum, the effects of an oxygen-rich seeding environment are pronounced,

Author contributions: M.L.Y. and Y.N. designed research; S.K., R.S.Y., E.N., P.C., and Y.N. performed research; Y.N. contributed new reagents/analytic tools; S.K., E.N., and Y.N. analyzed data; and M.L.Y. and Y.N. wrote the paper.

Conflict of interest statement: Dr. Eric Novik and Dr. Piyun Chao are employees of HuREL corporation.

This article is a PNAS Direct Submission.

[1]To whom correspondence should be addressed. E-mail: ynahmias@partners.org or ynahmias@cs.huji.ac.il.

This article contains supporting information online at www.pnas.org/cgi/content/full/0906820106/DCSupplemental.

www.pnas.org/cgi/doi/10.1073/pnas.0906820106

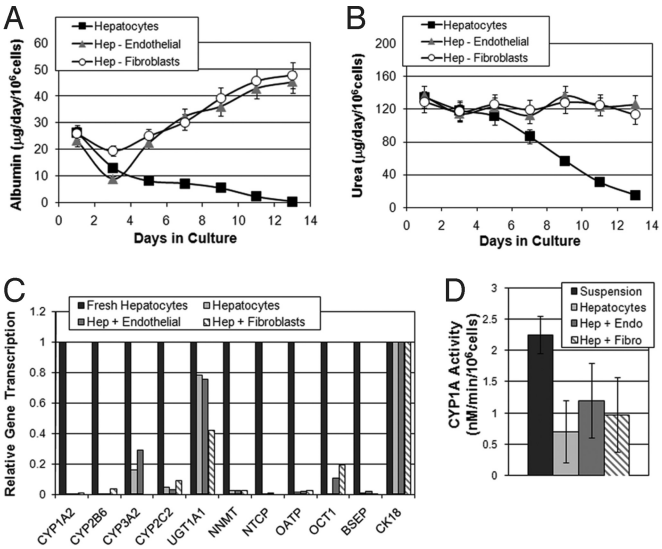

Fig. 1. Functional characterization of primary rat hepatocyte co-cultures with 3T3-J2 fibroblasts or endothelial cells. (*A*) Rates of albumin synthesis and (*B*) urea production over two weeks in culture and coculture. (*C*) Quantitative comparison of the transcription of phase I/II enzymes as well as influx and efflux transporters in hepatocytes cultured alone and those co-cultured with endothelial cells or 3T3-J2 fibroblasts (day 3) normalized to purified hepatic mRNA. UGT, UDP glycosyltransferase; NNMT, nicotinamide N-methyltransferase; NTCP, sodium-dependent bile acid transporter; OATP, organic anion transporting polypeptide; OCT, organic cation transporter; BSEP, bile salt export pump; CK18, cytokeratin 18. (*D*) Cyp1A1/2 activity in co-cultures of hepatocytes with endothelial cells or 3T3-J2 fibroblasts or those cultured alone (day 1) compared to freshly isolated hepatocytes in suspension (day 0). For additional details see *SI Materials and Methods*.

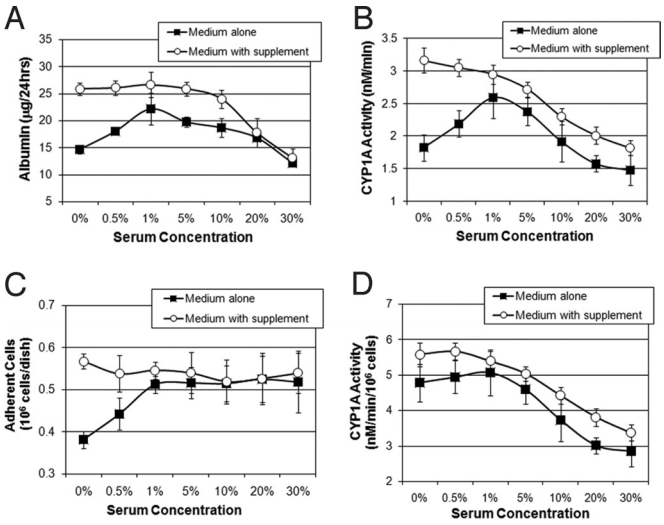

Fig. 2. Serum has a predominantly negative effect on the function of primary rat hepatocytes. (*A*) Rates of albumin synthesis and (*B*) Cyp1A1/2 activity following overnight seeding in serum-free media containing increasing concentrations of HI-FBS. (*C*) Total protein analysis demonstrates increased cell attachment with serum up to 1% concentration. In the presence of defined attachment supplement (with supplement) cellular attachment is decoupled from serum. (*D*) Cyp1A1/2 activity normalized to number of adhered cells, hepatocyte metabolic function is seen to be inversely correlated with serum content in the seeding media.

resulting in high levels of phase I/II metabolism, transporter activity, functional polarization and gene transcription from the onset and during long-term culture. This sustained metabolic competence allows for a critical evaluation of drug clearance rates, transporter activity, and drug-drug interactions for both slow and fast clearing drugs. Metabolic activity in oxygenated co-cultures is comparable and in many cases superior to suspension cultures, requires no adaptation period and is therefore associated with significantly reduced labor and cost.

Results

Minimal Gene Expression and Function During the Onset of Hepatocyte Culture. Fig. 1 *A* and *B* show albumin and urea production rates in primary rat hepatocytes co-cultured with 3T3-J2 fibroblasts or endothelial cells, compared to those cultured alone. Standard serum-containing hepatocyte culture medium was used for all culture conditions (9, 14). As was previously shown, a 3-day lag period occurs at the onset of culture during which albumin production is minimal. Supported by non-parenchymal cells, albumin synthesis slowly increases over time to stabilize around 46 μg/10^{6}cells/24 h by day 11. At the same time, hepatocytes cultured alone rapidly lose albumin and urea production. Quantitative gene expression analysis reveals that despite functional recovery in coculture, both culture configurations have markedly lower mRNA levels than freshly isolated cells at the onset of culture (Fig. 1*C*). We show that the expression of phase I and phase II enzymes as well as drug transporter proteins on day 3 of culture is significantly lower than in vivo for all culture configurations. As expected, Cyp1A activity measured by the EROD assay for co-cultures and monocultures was respectively 70 ± 20% and 50 ± 20% lower than hepatocytes in suspension (Fig. 1*D*).

Serum Has a Detrimental Effect on Short-Term Hepatocyte Function. Primary cells are thought to require significant adaptation to serum (23). To evaluate the effect of serum on the function of primary hepatocytes, primary rat hepatocytes were seeded at a density of 100,000 cells/cm^2 on collagen-coated plates in serum-free medium supplemented with increasing concentrations of heat-inactivated FBS. Fig. 2*A* shows albumin production during the first 24 h of culture, while Fig. 2*B* shows Cyp1A activity following 24 h of culture. Both albumin secretion and Cyp1A activity significantly increased with serum up to 1% concentration by 52 ± 8% ($P = 0.001$, $n = 3$) and 30 ± 10% ($P = 0.021$, $n = 3$), respectively. However, higher concentration of serum led to a significant decrease in albumin secretion and Cyp1A activity by 45 ± 4% ($P = 0.017$, $n = 3$) and 43 ± 1% ($P = 0.001$, $n = 3$), respectively. As cellular attachment is thought to be mediated by serum, we quantified cell attachment by measuring total protein as a surrogate measure of cell number which is linearly correlated with DNA content and cell counting in primary hepatocyte cultures (Fig. S1). Fig. 2*C* shows that cell adhesion increased in the presence of serum up to 1% concentration corresponding to the increased function. To compensate for this loss in cell adhesion, we supplemented the serum-free media with HμREL defined attachment supplement. Fig. 2*C* shows that in the presence of the attachment supplement, serum had little effect on cellular adhesion. More importantly, under these conditions Cyp1A activity increased by 74 ± 4% ($P = 0.020$, $n = 3$), Fig. 2*B*. Normalizing albumin production and Cyp1A activity to adherent cell number demonstrates that serum has a predominately negative effect on hepatocyte function during the first 24 h of culture (Fig. 2*D*).

Oxygenated Co-Cultures Support High Levels of Cyp1A1/2 and Cyp2B1/2 Activity. Oxygen is an important component of the hepatic microenvironment (15). While passive diffusion of oxygen is not thought to be limiting during normal culture (15), it fails to supply the oxygen requirements of primary rat and pig hepatocytes during the first 24 h of culture when oxygen

Table 1. Cyp1A activity in rat hepatocytes after 24 h of culture (nanomolar per minute per 10^6 cells)

	Hepatocytes		Hepatocyte - Endothelial	
	Serum free	10% Serum	Serum free	10% Serum
Normal oxygen	1.48 ± 0.12	0.70 ± 0.50	1.45 ± 0.35	1.20 ± 0.60
High oxygen	2.44 ± 0.20	0.89 ± 0.30	3.45 ± 0.21	1.29 ± 0.13

demands are three to four times higher than their basal levels (17, 18). Therefore, seeding primary hepatocytes under a partial pressure of 95% oxygen can potentially reduce the stress associated with the transition from in vivo to in vitro culture, supporting superior survival and metabolic function. Table 1 shows Cyp1A activity in monocultures and co-cultures of primary rat hepatocytes seeded overnight in 21% or 95% oxygen, corresponding to 7 or 32 mg/L oxygen at the air-liquid interface respectively. Both cultures were stabilized to atmospheric levels of oxygen for 30 min prior to the EROD assay to ensure basal levels of activity. Cyp1A activity was markedly elevated following culture in 95% oxygen. Monocultures activity was increased by 64%±8% while activity in co-cultures increased by 138 ± 6%. Interestingly, this increase in function could not be detected when the cells were cultured in the presence of 10% serum. Similar results were observed in monocultures and co-cultures of human hepatocytes (Table S1). Hepatocyte viability in co-cultures at 24 h was also significantly increased from 84 ± 4% at normal oxygen tension to 96 ± 2% at high oxygen tension ($P = 0.005$ $n = 3$) (Fig. S2). To further characterize the metabolic competence of co-cultures seeded in 95% oxygen, we quantified the activities of CYP1A1/2 and CYP2B1/2 enzymes in both rat and human cells. Fig. 3*A* compares Cyp1A1/2 and Cyp2B1/2 activity in primary rat hepatocytes co-cultured with endothelial cells in 95% oxygen for 24 h (day 1) to the activity of rat hepatocytes from the same isolation in suspension (day 0). Similar results are reproduced in Fig. S3 for cryopreserved human hepatocytes. Our data demonstrates that both human and rat oxygenated co-cultures support high levels of CYP450 activity, comparable to that of hepatocytes from the same isolation cultured in suspension.

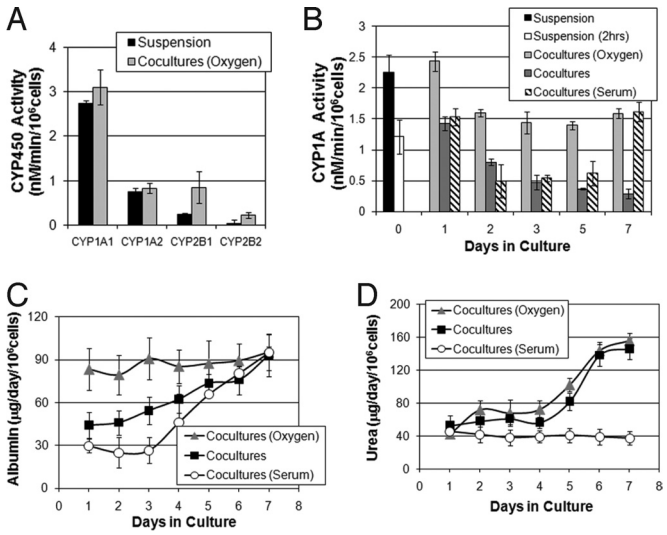

Fig. 3. Long-term function of serum-free oxygenated rat hepatocyte-endothelial co-cultures. (*A*) Activity of Cyp1A1/2 and Cyp2B1/2 in oxygenated co-cultures on the first day of culture (day 1) compared to hepatocytes from the same isolation cultured in suspension (day 0). (*B*) Long-term maintenance of Cyp1A1/2 activity in all three co-cultures compared to that of freshly isolated hepatocytes in suspension (Suspension). To account for the rapid loss of function in suspension, a second measurement was carried out on freshly isolated cells following 2 h of culture at 37 °C. (*C*) Rates of albumin synthesis and (*D*) urea production in serum-free hepatocyte-endothelial co-cultures seeded under normal oxygen tension (Cocultures) or 95% oxygen [Cocultures (Oxygen)]. Rates are compared to hepatocytes-endothelial co-cultures maintained in serum-containing culture medium [Cocultures (Serum)]. Synthetic activity in oxygenated co-cultures is maintained from the onset of culture.

Long-Term Maintenance of Hepatic Metabolic Competence in Oxygenated Co-Cultures. To further characterize the potential of oxygenated co-cultures we quantified albumin synthesis, urea production, and Cyp1A activity over 7 days in culture. Co-cultures of hepatocytes with endothelial cells were seeded in serum-free culture media under normal oxygen tension (co-cultures) or 95% oxygen [co-cultures (oxygen)]. As a second control representing widely used culture configuration we co-cultured hepatocytes with endothelial cells in serum-containing culture medium [co-cultures (serum)]. Fig. 3*C* demonstrates that albumin secretion during the first day of culture in 95% oxygen was 3-fold higher compared to serum-cultured cells ($P = 0.016$, $n = 3$), and 2-fold higher compared to serum-free cultured cells ($P = 0.049$, $n = 3$). No significant differences were detected by day 7. Interestingly, while urea production (Fig. 3*D*) was not statistically different at the onset of culture, it increased by day 7 in co-cultures seeded in 95% oxygen to be 4-fold higher than serum-cultured cells ($P = 0.001$, $n = 3$), but was not statistically different from the serum-free condition ($P = 0.057$, $n = 3$). To compare long-term Cyp1A activity to current model systems, we carried out two suspension measurements, one with freshly isolated hepatocytes and another with isolated hepatocytes following 2 h of incubation at 37 °C to account for the rapid loss of function in suspension. As shown above Fig. 3*B* demonstrates that Cyp1A activity in co-cultures seeded under high oxygen tension was comparable to that of hepatocytes in suspension. During the first day of culture, the activity was 59% higher than that of serum-cultured cells ($P = 0.001$, $n = 3$), and 70% higher than serum-free cultured cells ($P = 0.001$, $n = 3$). However, at day 7 of culture, there was no significant difference between the co-cultures suggesting similar levels of metabolic competence. Long-term metabolic and synthetic activity was further supported by microscopy. Fig. 4*B* demonstrates that oxygenated co-cultures of primary human hepatocytes retain their distinct polygonal morphology through day 9 of culture.

Gene Expression and Functional Polarization in Oxygenated Co-Cultures. To expand the characterization of oxygenated co-cultures we carried out gene expression analysis of phase I/II enzymes as well as drug transporters in both rat and human hepatocytes. As gene transcription of human hepatocytes is more clinically relevant it is presented in Fig. 4*A*, while rat data are shown in Fig. S4. Gene transcription of human hepatocytes following 24 h of culture was compared to mRNA isolated from the cryopreseved hepatocytes stock. Fig. 4*A* demonstrates that oxygenated co-cultures maintain a remarkable level of gene transcription following the first day of culture, comparable to in vivo levels of transcription. This result stands in contrast to the gene transcription levels of hepatocytes in serum-containing co-cultures which show dramatically lower levels of gene expression. To evaluate the functional activity of drug transporters in co-cultures seeded in 95% oxygen we stained human hepatocyte in oxygenated co-cultures with CDFDA, a compound which is metabolized into a fluorescent marker, and transported by polarized cells via MRP2 into bile canaliculi (25). Fig. 4*C* demonstrates that human hepatocytes seeded in 95% oxygen form functional bile canaliculi at the onset of culture. Another aspect of hepatocyte polarity is the presence of 3-O-sulfated heparan sulfate (HS4C3) on the basal surfaces of the cells (26). Heparan sulfate plays a critical role in the clearance of lipoproteins which are thought to

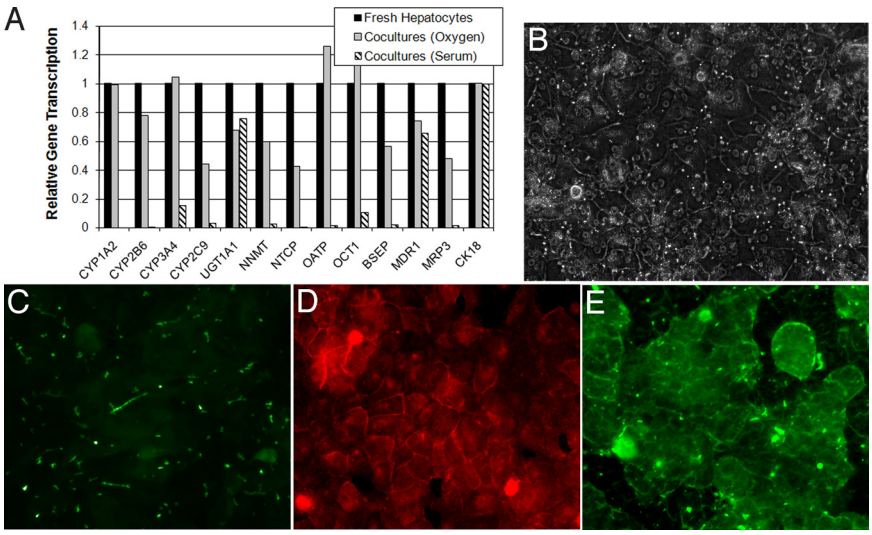

Fig. 4. Relative gene transcription and functional polarization in cultures of primary hepatocytes. (*A*) Quantitative comparison of the transcription of phase I/II enzymes as well as influx and efflux transporter in serum-free human hepatocyte-endothelial co-cultures seeded in 95% oxygen [Cocultures (Oxygen)] and those seeded in serum-containing medium [Cocultures (Serum)] following 1 day of culture compared to purified hepatic mRNA. MDR1/P-gp, multidrug resistance protein 1; MRP3, multidrug resistance protein 3. (*B*) Phase micrograph of primary human hepatocytes in oxygenated co-cultures following 9 days of culture. (*C*) Phase 3 transporter activity in oxygenated co-cultures of cryopreserved human hepatocytes (day 3). CDFDA is internalized by hepatocytes, cleaved by intracellular esterases and excreted into bile canaliculi as fluorescent CDF by active MRP2. (*D*) Immunofluorescence micrograph of 3-O-sulfated heparan sulfate (HS4C3) a liver specific proteoglycan found on the basal surface of rat hepatocytes in oxygenated co-cultures. Liver-specific heparan sulfate plays a critical role in the clearance of lipoproteins. (*E*) Immunofluorescence micrograph of the small leucine-rich proteoglycan, decorin, previously shown to be important in hepatocyte function. For additional images see Fig. S5.

be involved the transport and metabolism of several hydrophobic drugs (27, 28). Fig. 4*D* demonstrates basal surface staining for HS4C3 in co-cultures of primary rat hepatocytes (26). Finally, the small leucine-rich proteoglycan, decorin, which was previously shown to be important in the long-term maintenance of hepatocyte function can be also detected in oxygenated co-cultures (29). For additional images see Fig. S5.

Prediction of Drug Clearance Rates in Oxygenated Co-Cultures. The ability of a given culture system to predict in vivo drug metabolism is dependent on the activity of drug transporters, presence of appropriate phase I and II metabolic enzymes, and the efflux of metabolites. As such, time-dependant drug clearance provides a critical evaluation of the metabolic competence of the cells. Table S2 shows a list of drugs that were evaluated using our system. These include both fast and slow clearing drugs such as buspirone (CYP2D6, 3A4), timolol (CYP2D6), and carbamazepine (CYP3A4). Fig. 5 *A* and *B* show the in vitro clearance profiles of buspirone, metoprolol, timolol, sildenafil, antipyrine, and carbamazepine by co-cultures of primary rat hepatocytes seeded under high oxygen tension. All cultures were equilibrated in atmospheric oxygen for 30 min before drug addition to exclude enhanced metabolism driven by the participation of oxygen in the monooxygenation reaction. In vitro clearance of the same compounds by oxygenated co-cultures of cryopreserved human hepatocytes is shown in Fig. S6. Fig. 5 *A* and *B* demonstrate strong clearance of all test compounds. Comparing in vitro rates of drug clearance in oxygenated co-cultures of cryopreserved human hepatocytes to in vivo rates of hepatic clearance (30) shows a linear relationship with an R^2 of 0.92 (Fig. 5*E*) equivalent to the predictive ability of hepatocytes in suspension (Fig. 5*F*) with an R^2 of 0.91. We note some advantage in the detection of the clearance of slow-clearing drugs (Table S3)

Evaluating the Role of Transporters and Drug-Drug Interactions. Drug transporters, such as oatp2 and mdr1 (P-gp), play an important role in xenobiotic clearance as a necessary step before phase I metabolism (31, 32). Both drug transport and metabolism are known to be affected by the activities of co-administered drugs or dietary supplements with potentially disastrous consequences (32, 33). To demonstrate that oxygenated co-cultures can detect these drug-drug interactions we quantified the clearance of midazolam and digoxin in the presence of 100 μM of the oatp2 inhibitor rifampicin (31) or in the presence of 200 μM of the grapefruit flavonoid naringenin, a CYP3A4 and P-gp inhibitor (34–36). Fig. 5*C* shows the clearance of midazolam, a CYP3A4 substrate (37). The time course clearance of midazolam and the formation of its CYP3A4 metabolite 1′-OH-midazolam is demonstrated in oxygenated co-cultures of cryopreserved human cells (Fig. S6). Here we show that the clearance of midazolam is strongly inhibited by the naringenin but is unaffected by rifampicin as drug uptake is not mediated by oatp2. On the other hand, Fig. 5*D* shows the clearance of digoxin, a rat CYPA4 substrate dependent on oatp2-mediated uptake (31). Digoxin clearance is strongly inhibited by both naringenin and rifampicin.

Discussion

The liver is a major site for the metabolism of both endogenous and exogenous compounds due to its abundant levels of phase I/II enzymes (38). For this reason, major efforts are focused on evaluating drug clearance and other pharmacokinetic parameters of new chemical entities (2, 3). Currently, drug discovery and preclinical development programs are plagued by unreliable models and escalating costs. One retrospective study of 68 randomly selected investigational drugs estimated that a 12% improvement in preclinical screens or a 50% reduction in screening time could reduce total cost of drug development by over $200 million per drug (39, 40). The development of such rapid and predictive preclinical screens requires the engineering of new systems in which primary hepatocyte maintain a high level of metabolic competence with a minimal adaptation period.

One such system is described in this work, where we demonstrate that the combination of a serum-free culture environment with cell seeding at 95% oxygen supports a remarkable level of liver specific synthetic and metabolic activity, gene expression, and functional polarization in both rat and human hepatocytes. Oxygenated co-cultures supported gene expression profiles on par with in vivo levels of hepatic mRNA, and cytochrome P450 activity levels (1A1/2, 2B1/2, 3A4, and 2D6) equivalent or superior to freshly isolated hepatocytes. We have also demonstrated the activity of the basal/sinusoidal influx transporter oatp2, and the apical efflux transporter MRP2. These co-cultures seeded under high oxygen tension showed a similar ability to predict in vivo hepatic clearance of both rapid and slow clearing drugs with an R^2 of 0.92 compared to 0.91 for hepatocytes in suspension, although we note that the actual value of such in vitro vs. in vivo comparison is uncertain. Moreover, as function in oxygenated co-cultures does not require 7 to 10 days to stabilize (6, 14), this culture technique significantly reduces overall labor and cost. During this work we identified no clear

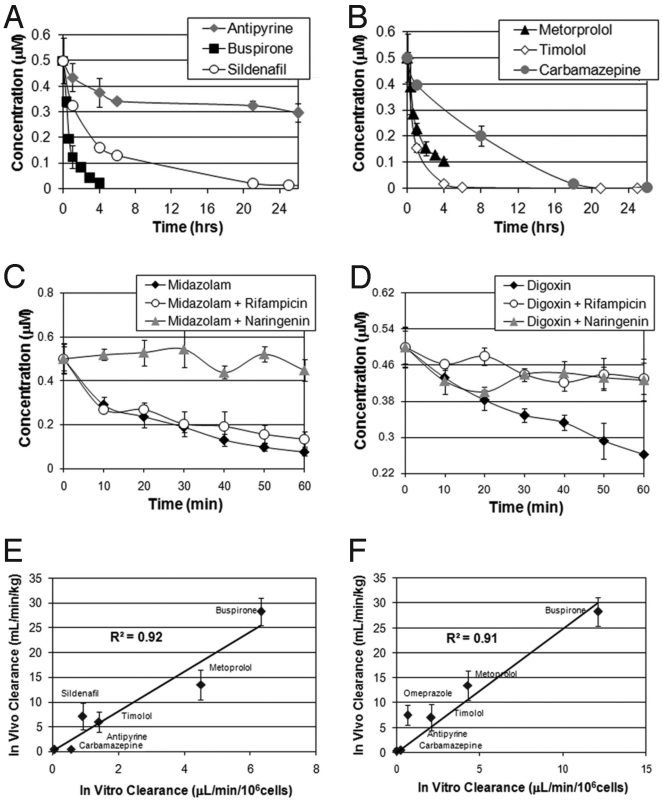

Fig. 5. Drug clearance and functional characterization of oxygenated co-cultures. (*A* and *B*) time course studies of the primary rat hepatocyte metabolism of rapidly clearing drugs, buspirone and metoprolol, medium clearing drugs, timolol and sildenafil, and slow clearing drugs, antipyrine and carbamazepine. (*C*) Time course of the metabolism of midazolam by oxygenated rat co-cultures following incubation with the oatp2 inhibitor rifampicin (100 μM) or the CYP3A4 and Pgp inhibitor naringenin (200 μM). (*D*) Time course of the metabolism of digoxin by oxygenated rat co-cultures following incubation with the oatp2 inhibitor rifampicin (100 μM) or the CYP3A4 and Pgp inhibitor naringenin (200 μM). (*E*) Comparison of in vitro rates of drug clearance measured in oxygenated co-cultures of cryopreserved human hepatocytes (day 1) with previously reported in vivo rates of hepatic clearance. The results are in excellent agreement with an R^2 of 0.92. (*F*) Comparison of in vitro rates of drug clearance measured in suspension cultures of cryopreserved human hepatocytes (day 0) with previously reported in vivo rates of hepatic clearance. For time course study in human cells see Fig. S6.

advantage of using endothelial cells over mouse 3T3-J2 fibroblasts, other than endothelial cells being species-specific. Therefore our results are readily extendable to other culture configurations including microfabricated co-cultures (14).

A significant element of our system is the serum-free media formulation. Such hormonally defined medium was originally reported to support gene transcription and gap junction communication in primary rat hepatocytes (23, 24). However, these serum-free cultures are traditionally carried out following cell seeding in serum-containing media. Here we demonstrate that the effects of serum are detrimental for hepatocyte function, even during a short overnight cell seeding. We suggest that positive effects of serum are mainly due to its ability to enhance cellular attachment, even on collagen-coated dishes. Enhancing cellular attachment in the absence of serum results in a significant increase in function and opens the door for oxygen-mediated enhancement.

While the transition to serum-free media demonstrated an increase in function, it is the transition to 95% oxygen that allowed the full metabolic potential of co-cultures to be realized. In vivo a mixture of venous and arterial blood supplies oxygen to hepatocytes at a rate of 1.2 nmol/s/10^6 cells (7). Fittingly, our prior work demonstrated that oxygen consumption of primary hepatocyte is 0.9 nmol/s/10^6 cells during the first 24 h of culture (17). However, as the cells adapt to their new microenvironment, oxygen uptake rates drop to 0.4 nmol/s/10^6 cells during long-term culture (17, 18). Not surprisingly, 0.4 nmol/s/10^6 cells is also the upper limit of oxygen diffusion under atmospheric oxygen, but significantly less than hepatocyte demand during seeding (16). Metabolic flux models also suggest that hepatocytes in culture attempt to maximize their oxygen uptake (41). This suggests the oxygen supply is a limiting factor in the metabolic activity of hepatocytes. Therefore, increasing oxygen tension to 95%, which allows for oxygen supply in excess of 1.2 nmol/s/10^6 cells to occur by passive diffusion, can reduce adaptation stress and allow for higher levels of metabolic activity.

Under these conditions, CYP1A activity, albumin secretion, and hepatocyte viability were, respectively, 70 ± 7%, 90 ± 18%, and 13 ± 5% higher in co-cultures seeded at 95% oxygen compared to co-cultures seeded at 21% oxygen. Drug clearance rates and gene transcription levels were similarly enhanced. These results stand in contrast to previous work which failed to find a significant enhancement of hepatocyte function at oxygen tensions greater than atmospheric (19, 21, 22). Our work clearly shows this is due to the effects of serum and in its presence the enhancement of function is minimal (Table 1 and Table S1). We note that oxygen supply is dependent on its rate of consumption and hence the global density of hepatocytes in culture. Reducing hepatocyte density to the point where oxygen is no longer limiting can have a similar effect to increasing oxygen tension. The Cho et al. demonstration of elevated oxygen uptake rates and enhanced synthetic function in low density cultures of rat hepatocytes supports this assertion (42). However, homotypic interactions are important in the maintenance of hepatocyte function, requiring the maintenance of high local cell density while global cell density is decreased. Micropatterned hepatocyte co-cultures, recently shown to support high levels of metabolic activity correspond to such a configuration. It may be interesting to test whether the elevated long-term activity in micropatterned cultures is due to increased oxygen availability.

The ability to quantify rates of hepatic clearance in a rapid and cost efficient manner represents a major advancement to the current state-of-the-art. Our work demonstrated that hepatocytes co-cultured under 95% oxygen demonstrate high levels of metabolic activity. In addition, long-term function allows the critical evaluation of slow clearing drugs as well as drug-drug interactions without the requirement for a long, work-intensive adaptation period. The functional polarization of the cells, demonstrated by active transporters, and proteoglycan expression, suggests this culture model can be particularly useful in the study of complex transporter dependent drug metabolism and perhaps even viral infection.

Materials and Methods

Hepatocyte Isolation and Culture. Primary rat hepatocytes were harvested from adult female Lewis rats purchased from Charles River Laboratories, weighing 150–200 g by a two-step in situ collagenase perfusion technique, modified by Dunn et al. 1991 (43). Hepatocyte viability after harvest was greater than 90% and purity was greater than 95%. All animals were treated in accordance with National Research Council guidelines and approved by the Subcommittee on Research Animal Care at the Massachusetts General Hospital. Primary human hepatocytes were obtained from BD Biosciences or were kindly provided by Dr. Stephen C. Strom, University of Pittsburgh. Cryopreserved human hepatocytes were purchased from either BD Biosciences or Celsis. Human cells were purified in 33% Percoll solution centrifuged at 500 × *g* for 5 min before seeding. Cell viability post purification was greater than 90% and purity greater than 95%. Following purification hepatocytes were suspended in ice cold culture medium at 1 × 10^6 cells/mL and seeded on collagen-coated 6-, 12-, or 96-well plates as described. Unless otherwise noted seeding densities were 150,000 cells/cm^2. Hepatocyte cultures were main-

tained at 37 °C, 5% CO_2 humidified incubator at varying partial pressures of oxygen as indicated in the text. Suspension cultures were carried out on freshly isolated cells in microcentrifuge tubes at a density of 1×10^6 cells/mL. Suspensions were maintained under constant shacking at 37 °C.

Non-Parenchymal Cells. 3T3-J2 mouse embryonic fibroblasts were obtained from Dr. Howard Green, Department of Cellular and Molecular Physiology, Harvard Medical School, and cultured as previously described (44). Primary rat cardiac microvascular endothelial cells (RCEC) and primary human lung microvascular endothelial cells were purchased from VEC Technologies and Lonza Inc., respectively. Endothelial cells were cultured in microvascular Endothelial Growth Medium (EGM2mv) purchased from Lonza, split when 80% confluent, and used before passage eight. Human endothelial cells were used with human hepatocytes and rat endothelial cells were used with rat hepatocytes.

Hepatocyte Culture Medium. Conventional serum-containing hepatocyte medium was composed of DMEM basal medium, supplemented with 10% HI-FBS, 0.5 U/mL insulin, 20 ng/mL epidermal growth factor (EGF), 7 ng/mL glucagon, 7.5 mg/mL hydrocortisone, and 1% penicillin-streptomycin. Alternatively, hepatocytes were cultured in a proprietary HμREL serum-free medium composed of a basal medium supplemented with ascorbic acid, insulin, transferrin, EGF, and antibiotics. This serum-free medium was further supplemented with HμREL defined attachment supplement during the hepatocyte seeding stage as is indicated in the text.

Generation of Oxygenated Cultures. Oxygenated cultures and co-cultures were generated by introducing 95% oxygen and 5% CO_2 gas mixture (Airgas) into a 37 °C humidified incubator and allowing the atmosphere to equilibrate for at least 1 h before cell seeding. At these partial pressures we estimate the concentration of oxygen at the air-liquid interface to be approximately 7 mg/L at 21% oxygen, and 32 mg/L at 95% oxygen. Following overnight cell seeding under 95% oxygen the cultures were washed and allowed to equilibrate to atmospheric oxygen for 30 min before any measurements of CYP450 activity as oxygen actively participates in the reaction. In our hands, oxygen concentration stabilizes in under 20 min.

Statistical Analysis. Results are reported as mean ± standard deviation. N denotes the number of experimental replicates. Statistical analysis was performed using a Student's t test, with $P < 0.05$ considered to be significant.

ACKNOWLEDGMENTS. We thank Carley J. Shulman and Chris Pohun Chen for technical support. This work was supported by National Institutes of Health/National Institute of Diabetes and Digestive and Kidney Diseases Grant K01DK080241, National Institutes of Health BioMEMS Resource Center Grant P41 EB-002503, and the Shriners Hospital.

1. Kaplowitz N (2005) Idiosyncratic drug hepatotoxicity. *Nat Rev Drug Discov* 4:489–499.
2. Ballet F (1997) Hepatotoxicity in drug development: Detection, significance, and solutions. *J Hepatol* 26:26–36.
3. Pritchard JF, et al. (2003) Making better drugs: Decision gates in non-clinical drug development. *Nat Rev Drug Discov* 2:542–553.
4. Lau YY, Sapidou E, Cui X, White RE, Cheng K-C (2002) Development of a novel in vitro model to predict hepatic clearance using fresh, cryopreserved, and sandwich-cultured hepatocytes. *Drug Metab Dispos* 30:1446–1454.
5. Gebhardt R, et al. (2003) New hepatocyte in vitro systems for drug metabolism: Metabolic capacity and recommendations for application in basic research and drug development, standard operation procedures. *Drug Metab Rev* 35:145–213.
6. Yarmush ML, et al. (1992) Hepatic tissue engineering. Development of critical technologies. *Ann N Y Acad Sci* 665:238–252.
7. Nahmias Y, Berthiaume F, Yarmush ML (2006) Integration of technologies for hepatic tissue engineering. In *Advances in Biochemical Engineering/Biotechnology*, eds Lee K, Kaplan D (Springer Berlin, Heidelberg), Vol 103, pp 309–329.
8. Bhatia SN, Balis UJ, Yarmush ML, Toner M (1999) Effect of cell-cell interactions in preservation of cellular phenotype: Cocultivation of hepatocytes and non parenchymal cells. *FASEB J* 13:1883–1900.
9. Dunn JC, Yarmush ML, Koebe HG, Tompkins RG (1989) Hepatocyte function and extracellular matrix geometry: Long-term culture in a sandwich configuration. *FASEB J* 3:174–177.
10. Dunn JC, Tompkins RG, Yarmush ML (1992) Hepatocytes in collagen sandwich: Evidence for transcriptional and translational regulation. *J Cell Biol* 116:1043–1053.
11. Landry J, Bernier D, Ouellet C, Goyette R, Marceau N (1985) Spheroidal aggregate culture of rat liver cells: Histotypic reorganization, biomatrix deposition, and maintenance of functional activities. *J Cell Biol* 101:914–923.
12. Bhatia SN, Yarmush ML, Toner M (1997) Controlling cell interactions by micropatterning in co-cultures: Hepatocytes and 3T3 fibroblasts. *J Biomed Mater Res* 34:189–199.
13. Morin O, Normand C (1986) Long-term maintenance of hepatocyte functional activity in co-culture: Requirements for sinusoidal endothelial cells and dexamethasone. *J Cell Physiol* 129:103–110.
14. Khetani SR, Bhatia SN (2007) Microscale culture of human liver cells for drug development. *Nat Biotechnol*:doi:10.1038/nbt1361.
15. Stevens KM (1965) Oxygen requirements for liver cells in vitro. *Nature* 206:199.
16. Nahmias Y, et al. (2006) A novel formulation of oxygen-carrying matrix enhances liver-specific function of cultured hepatocytes. *FASEB J* 20:2531–2533.
17. Balis UJ, et al. (1999) Oxygen consumption characteristics of porcine hepatocytes. *Metab Eng* 1:49–62.
18. Rotem A, Toner M, Tompkins RG, Yarmush ML (1992) Oxygen uptake rates in cultured rat hepatocytes. *Biotechnol Bioeng* 40:1286–1291.
19. Rotem A, et al. (1994) Oxygen is a factor determining in vitro tissue assembly: Effects on attachment and spreading of hepatocytes. *Biotechnol Bioeng* 43:654–660.
20. Tilles AW, Baskaran H, Roy P, Yarmush ML, Toner M (2001) Effects of oxygenation and flow on the viability and function of rat hepatocytes cocultured in a microchannel flat-plate bioreactor. *Biotechnol Bioeng* 73:379–389.
21. Yanagi K, Ohshima N (2001) Improvement of metabolic performance of cultured hepatocytes by high oxygen tension in the atmosphere. *Artificial Organs* 25:1–6.
22. Suleiman SA, Stevens JB (1987) The effect of oxygen tension on rat hepatocytes in short-term culture. *In Vitro Cell* Dev Biol 23:332–338.
23. Enat R, et al. (1984) Hepatocyte proliferation in vitro: Its dependence on the use of serum-free hormonally defined medium and substrata of extracellular matrix. *Proc Natl Acad Sci USA* 81:1411–1415.
24. Fujita M, et al. (1987) Glycosaminoglycans and proteoglycans induce gap junction expression and restore transcription of tissue-specific mRNAs in primary liver cultures *Hepatology* 7:1S–9S.
25. Turncliff RZ, Tian X, Brouwer KLR (2006) Effect of culture conditions on the expression and function of Bsep, Mrp2, and Mdrla/b in sandwich-cultured rat hepatocytes. *Biochem Pharmacol* 71:1520–1529.
26. Dam GB, et al. (2006) 3-O-Sulfated oligosaccharide structures are recognized by anti-heparan sulfate antibody HS4C3. *J Biol Chem* 281:4654–4662.
27. Wasan KM, Brocks DR, Lee SD, Sachs-Barrable K, Thornton SJ (2008) Impact of lipoproteins on the biological activity and disposition of hydrophobic drugs: Implications for drug discovery. *Nat Rev Drug Discov* 7:84–99.
28. MacArthur JM, et al. (2007) Liver heparan sulfate proteoglycans mediate clearance of triglyceride-rich lipoproteins independently of LDL receptor family members. *J Clin Invest* 117:153–164.
29. Khetani SR, Szulgit G, Rio JAD, Barlow C, Bhatia SN (2004) Exploring interactions between rat hepatocytes and nonparenchymal cells using gene expression profiling. *Hepatology* 40:545–554.
30. Thummel KE, Shen DD, Isoherranen N, Smith HE (2005) Appendix II. Design and Optimization of Dosage Regimens: Pharmacokinetic Data. In *Goodman & Gilman's The Pharmacological Basis of Therapeutics*, ed Brunton LL (McGraw-Hill Professional), 11th Ed, pp 1984.
31. Lam JL, Benet LZ (2004) Hepatic microsome studies are insufficient to characterize in vivo hepatic metabolic clearance and metabolic drug-drug interactions: Studies of digoxin metabolism in primary rat hepatocytes versus microsomes. *Drug Metab Dispos* 32:1311–1316.
32. Benet LZ, Cumminsa CL, Wua CY (2004) Unmasking the dynamic interplay between efflux transporters and metabolic enzymes. *Int J Pharm* 277:3–9.
33. Custodio JM, Wu C-Y, Benet LZ (2008) Predicting drug disposition, absorption/elimination/transporter interplay and the role of food on drug absorption. *Adv Drug Deliv Rev* 60:717–733.
34. Jurima-rometa M, Huanga HS, Beckb DJ, Li AP (1996) Evaluation of drug interactions in intact hepatocytes: Inhibitors of terfenadine metabolism. *Toxicol in Vitro* 10:655–663.
35. Haehner T, Refaie MO, Müller-Enoch D (2004) Drug-drug interactions evaluated by a highly active reconstituted native human cytochrome P4503A4 and human NADPH-cytochrome P450 reductase system. *Arzneimittelforschung* 54:78–83.
36. Ho PC, Saville DJ, Wanwimolruk S (2001) Inhibition of human CYP3A4 activity by grapefruit flavonoids, furanocoumarins and related compounds. *J Pharm Pharm Sci* 4:217–227.
37. Benet LZ (2005) There are no useful CYP3A probes that quantitatively predict the in vivo kinetics of other CYP3A substrates and no expectation that one will be found. *Mol Interv* 5:79–83.
38. Murray KF, Messner DJ, Kowdley KV (2006) Mechanisms of hepatocyte detoxification. In *Physiology of the gastrointestinal tract*, ed Johnson LR (Academic), 4 Ed. Vol 1, pp 1483–1504.
39. DiMasi JA (2002) The value of improving the productivity of the drug development process: faster times and better decisions. *Pharmacoeconomics* 20:1–10.
40. DiMasi JA, Hansenb RW, Grabowskic HG (2003) The price of innovation: New estimates of drug development costs. *J Health Econ* 22:151–185.
41. Uygun K, Matthew HWT, Huang Y (2007) Investigation of metabolic objectives in cultured hepatocytes. *Biotechnol Bioeng* 97:622–637.
42. Cho CH, et al. (2007) Oxygen uptake rates and liver-specific functions of hepatocyte and 3T3 fibroblast co-cultures. *Biotechnol Bioeng* 97:188–199.
43. Dunn JCY, Tompkins RG, Yarmush ML (1991) Long-term in vitro function of adult hepatocytes in a collagen sandwich configuration. *Biotechnol Prog* 7:237–245.
44. Nahmias Y, Casali M, Barbe L, Berthiaume F, Yarmush ML (2006) Liver endothelial cells promote LDL-R expression and the uptake of HCV-like particles in primary rat and human hepatocytes. *Hepatology* 43:257–265.

Supporting Information

Kidambi et al. 10.1073/pnas.0906820106

SI Materials and Methods

Reagents and Antibodies. FBS, PBS, Dulbecco's Modified Eagle Medium (DMEM), penicillin, and streptomycin were obtained from Invitrogen Life Technologies. Human low density lipoprotein (LDL) was purchased from Biomedical Technologies. Insulin was obtained from Eli-Lilly. Immunofluorescence grade paraformaldehyde was purchased from Electron Microscope Sciences. Unless otherwise noted, all other chemicals were purchased from Sigma-Aldrich Chemicals. For immunofluorescence studies, normal donkey serum and secondary F(ab′)2 antibody fragments, ML grade, were obtained from Jackson Immunoresearch. Mouse anti-VSV glycoprotein (10 μg/mL) was purchased from Sigma-Aldrich, while Goat anti-Decorin (5 μg/mL) was purchased from R&D Systems. Phage display-derived single chain antibody against 3-O-sulfated heparan sulfate (HS4C3) was a kind gift of Dr. Arie Oosterhof, Radboud University Nijmegen Medical Center, Netherlands.

Quantification of Cell Adhesion. Following overnight incubation, culture medium was removed and the cells carefully washed with PBS to remove non-adherent cells. Adherent cells were then lysed in 0.1% Triton X-100 and total cellular protein was quantified using the Bio-Rad Bradford protein assay. Serum concentration did not affect this assay (Fig. S1).

Cytochrome P450 Activity. The activities of CYP1A1/2 and CYP2B1/2 were measured using the ethoxyresorufin-O-deethylase (EROD), methoxyresorufin-O-deethylase (MROD), penthoxyresorufin-O-deethylase (PROD), and benzyloxyresorufin-O-deethylase (BROD) assays respectively, as previously described (21). This assay measures uninduced basal levels of activity.

Albumin and Urea Analysis. Media samples were collected daily and stored frozen at −80 °C for subsequent analysis of albumin and urea content. Albumin concentration was measured by ELISA (ELISA). Urea synthesis was analyzed by a commercially available Blood Urea Nitrogen Assay Kit (Stanbio Laboratory).

Quantitative Reverse Transcriptase Polymerase Chain Reaction (qRT-PCR). RNA isolation was carried out using Clontech Laboratories NucleoSpin RNA II kit according to manufacturer instructions. RNA purity and concentration was quantified using NanoDrop ND-1000 spectrophotometer (Thermo Fisher Scientific). Bio-Rad iScript One-Step RT-PCR Kit was used to analyze gene expression. Reactions were initiated using 10 ng template RNA and 20 nM primers in 25 μL total volume on BioRad iCycler Real Time PCR in a 96-well plate format. Gene transcription was evaluated using the $\Delta\Delta C_t$ method normalized to cytokeratin 18 (CK18), an epithelial specific intermediate filament, and to RNA from freshly isolated hepatocytes.

Immunofluorescence Microscopy. Hepatocytes were washed with PBS and fixed in 4% EM-grade paraformaldehyde for 10 min at room temperature. Slides were then washed with PBS and incubated in 100 mM glycine for 15 min to saturate reactive groups. Samples were permeabilized for 15 min with 0.1% Triton X-100, blocked for 30 min with 1% BSA and 5% donkey serum at room temperature, and stained with primary antibodies overnight at 4 °C. After additional washes with PBS, samples were stained with fluorescently tagged secondary antibodies for 45 min at room temperature.

Bile Canaliculi Analysis. Functional bile canaliculi were detected by fluorescence microscopy following 10-min incubation with 2 μg/mL of 5 (6)-carboxy-2′,7′-dichlorofluorescein diacetate (CDFDA) (30). CDFDA passively diffuses into hepatocytes, where is it hydrolyzed to fluorescent carboxy-dichlorofluorescein (CDF). In polarized hepatocytes, CDF is transported via MRP2 into bile canaliculi. Non-polarized hepatocytes accumulate CDF and slowly release it to the media via MRP3.

Drug Clearance Studies. Buspirone, metoprolol, timolol, sildenafil, antipyrine, carbamazepine, digoxin, and midazolam were premixed with hepatocyte culture medium at a concentration of 0.5 μM and introduced to the oxygenated co-cultures (1×10^6 cells/mL) following an overnight incubation in 95% oxygen. All experiments were carried out at atmospheric oxygen to ensure basal levels of activity. Non-specific binding, degradation, and evaporation of the test drugs were quantified by carrying out identical experimental controls without cells. Ten-microliter samples were taken at specified time intervals and transferred to 200 μL methanol solution containing 10 ng/mL loperamide or carbamazepine as internal standards. Samples were then stored at −80 °C until analysis. Before analysis, samples were centrifuged at $1{,}000 \times g$ for 10 min and 10 μL supernatant was analyzed by LC-MS/MS. The LC-MS/MS system was comprised of a Shimadzu LC-10ADvp pump and an APT 4000 mass spectrometer with a Turbo Ion Spray probe (MDS SCIEX). Separation of compounds was achieved using a reversed phased stationary phase (Advantage ARMOR C-18, 5 μm, 30.0 × 2.1 mm, Analytical).

Drug-Drug Interactions. To explore drug transporter and enzymatic interactions between drugs we treated the oxygenated co-cultures with either 100 μM of rifampicin or 200 μM of the grapefruit flavonoid naringenin for 1 h before the addition of either digoxin or midazolam at 1 μM concentration. Ten-microliter samples were taken at 10-min time intervals for 60 min and transferred to 200 μL methanol solution containing 10 ng/mL loperamide internal standards. Samples were then analyzed by LC-MS/MS as described above.

Calculation of In Vitro Intrinsic Clearance. Intrinsic clearance (CL_{int}) values were calculated using the following formula (4):

$$CL_{\text{int}} = \frac{C_0 - C_{time}}{AUC_{0-time}} \cdot \frac{V}{N}$$

where C_0 and C_{time} are the concentrations of the drugs at the start and end of the experiment respectively given in μM, $AUC_{0\text{-}time}$ is area under the concentration versus time curve, V is the volume of incubation (500 μL), and N is the hepatocyte number. Intrinsic clearance values in μL/h/10^6 hepatocytes were compared to in vivo values of drug clearance (CL/F) obtained from Goodman & Gilman's Pharmacology (35) and adjusted for urinary excretion of the drug to assess an in vivo value of hepatic clearance.

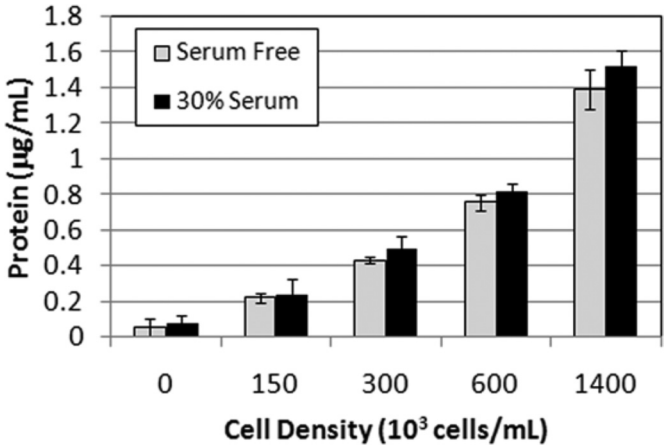

Fig. S1. Quantification of cell adhesion is unaffected by medium serum content. A calibration curve of total protein to known cell number was generated using freshly isolated cells. To generate the figure above, increasing concentrations of cells were seeded in the presence of attachment factors, in serum-free or 30% serum culture medium. Following overnight incubation, medium was removed and the cultures carefully washed to remove non-adherent cells. Adherent cells were lysed and total cellular protein was quantified using the Bradford method. Serum concentration did not affect the measurement.

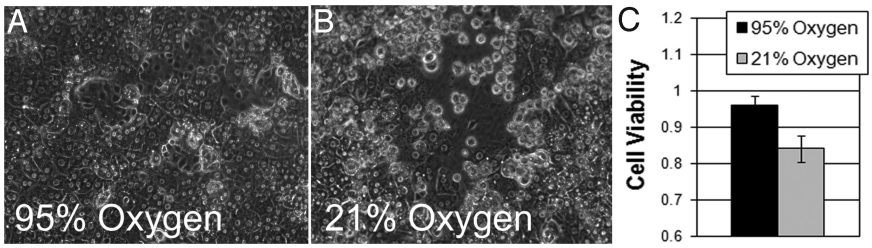

Fig. S2. Viability of primary rat hepatocytes following 24 hours of culture in serum-free medium under normal atmospheric oxygen (21%) or 95% oxygen. Hepatocytes were seeded at relatively high density (150,000 cells/cm^2). (*A* and *B*) Phase image micrographs of co-cultures indicating cell death under normal oxygen tensions. (*C*) Cell viability was quantified by measuring aspartate aminotransferase (AST) levels. AST is an intracellular enzyme released during hepatocyte death. AST levels were normalized to total amount of AST following total cell lysis in 0.1% triton.

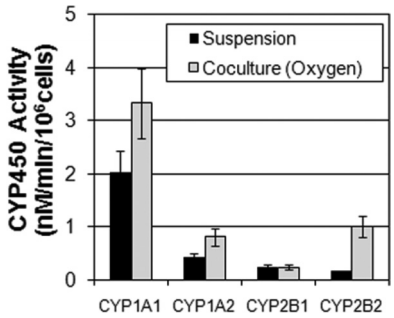

Fig. S3. Activity of CYP1A1/2 and CYP2B1/2 in co-cultures of cryopreserved human hepatocytes seeded in high oxygen tension on the first day of culture (day 1) measured by the deethylation of ethoxyresorufin (EROD), methoxyresorufin (MROD), penthoxyresorufin (PROD), and benzyloxyresorufin (BROD) respectively compared to hepatocytes from the same batch cultured in suspension (day 0). CYP1A1/2 and Cyp2B1/2 activity in is equivalent or greater than hepatocytes in suspension.

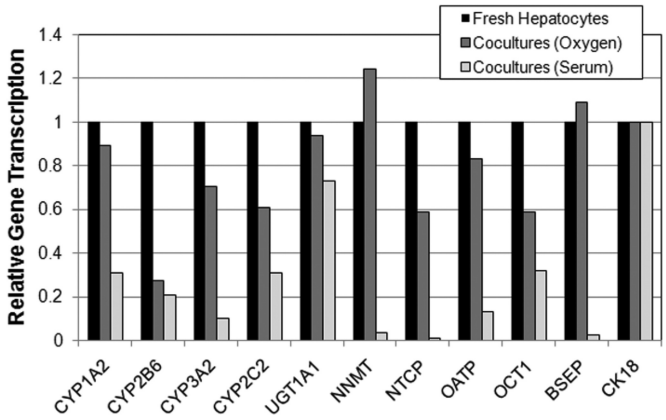

Fig. S4. Quantitative RT-PCR comparison of the transcription of phase I/II enzymes as well as influx and efflux transporter in serum-free co-cultures of primary rat hepatocyte seeded under high oxygen tension (Cocultures (Oxygen)) and those seeded in serum-containing medium (Cocultures (Serum)) following 1 day of culture compared to purified rat hepatic mRNA from the same animal.

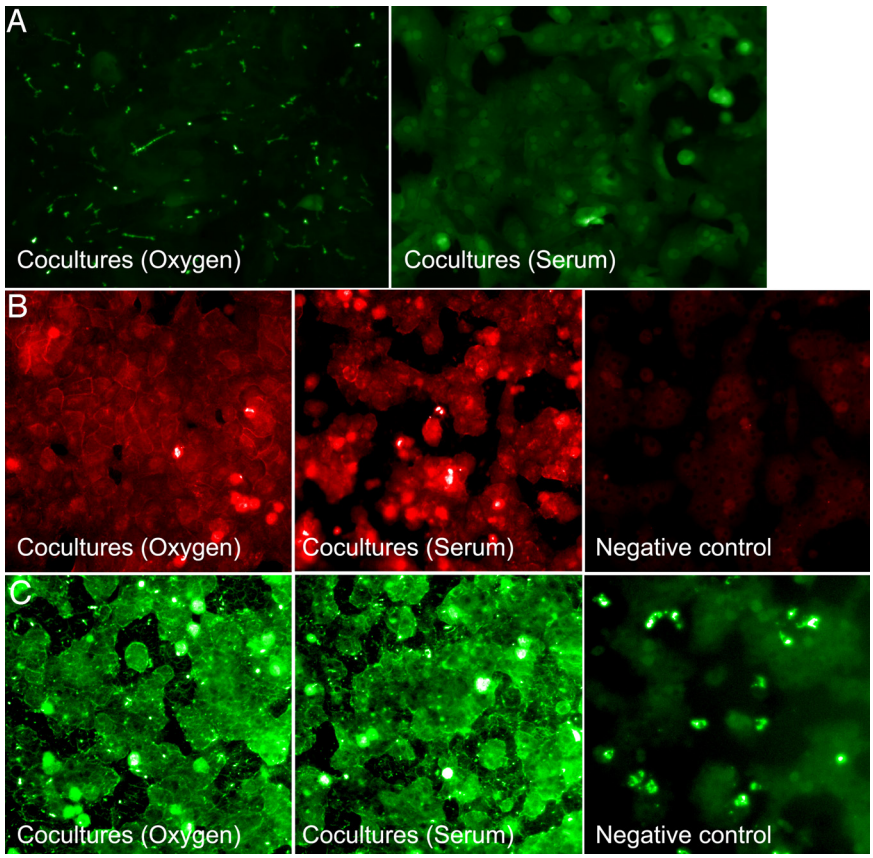

Fig. S5. (*A*) Phase 3 transporter activities in co-cultures of cryopreserved human hepatocytes cultured under high oxygen tension (Coculture (Oxygen)) or in the presence of serum (Coculture (Serum)) on day 3 of culture. CDFDA is internalized by hepatocytes, cleaved by intracellular esterases and excreted into bile canaliculi as fluorescent CDF by active MRP2. While MRP2 activity is present in co-cultures seeded under high oxygen tension, it appears to be absent from serum-containing co-cultures on day 3 of culture. (*B*) Immunofluorescence micrograph of 3-O-sulfated heparan sulfate (HS4C3) a liver specific proteoglycan found on the basal surface of rat hepatocytes. Liver-specific heparan sulfate plays a critical role in the clearance of lipoproteins. While HS4C3 is present in both culture conditions, the staining appears to be more extensive in co-cultures seeded under high oxygen tension. (*C*) Immunofluorescence micrograph of the small leucine-rich proteoglycan, decorin, previously shown to be important in hepatocyte function. Both culture conditions stain for decorin equally well.

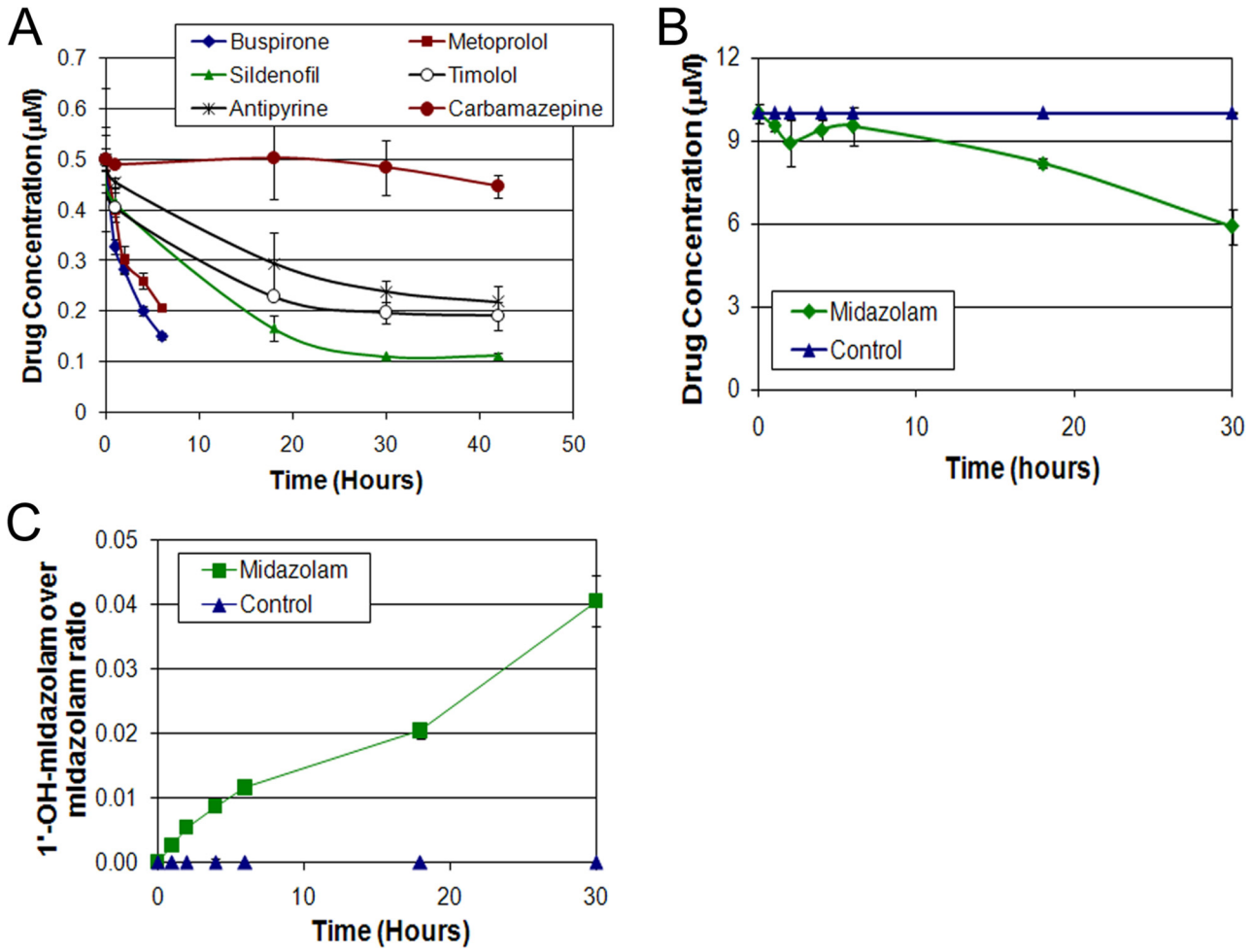

Fig. S6. Drug clearance profiles and metabolite formation generated in oxygenated co-cultures of cryopreserved human hepatocytes with 3T3-J2 fibroblasts. (*A*) Oxygenated co-cultures of cryopreserved human hepatocytes demonstrate the clearance of buspirone, metoprolol, sildenofil, timolol, antipyrine, and carbamazepine. (*B*) and (*C*) Human heptoacyte metabolism of 10 μM of midazolam was accompanied by clear formation of its CYP3A4 metabolite 1′-OH-midazolam. Values are presented as the ratio of 1′-OH-midazolam over midazolam.

Table S1. CYP1A activity in cryopreserved human hepatocytes following 24 hours of culture (nM/min/10^6 cells)

	Hepatocytes		Hepatocyte - Endothelial	
	Serum free	10% Serum	Serum free	10% Serum
Normal Oxygen	1.60 ± 0.61	1.42 ± 0.64	1.44 ± 0.13	0.90 ± 0.27
High Oxygen	2.10 ± 0.88	1.18 ± 0.91	2.79 ± 0.49	1.30 ± 0.77

Table S2. Phase I enzymes of drug targets

Drug	Phase I enzyme
Buspirone	CYP2D6, CYP3A4
Metoprolol	CYP2D6
Timolol	CYP2D6
Sildenafil	CYP3A4, CYP2C9
Carbamazepine	CYP3A4
Midazolam	CYP3A4,1
Antipyrine	CYP1A2, CYP2B6, CYP2C8,9,18 and CYP3A4

Table S3. In vivo / In vitro comparison of drug clearance in suspension (day 0) and oxygenated co-cultures of cryopreserved human hepatocytes (day 1)

Drug	In Vivo Clearance (mL/min/kg)	Urinary excretion (%)	Suspension culture, μL/min/10^6 cells	Oxygenated Co-culture, μL/min/10^6 cells
Buspirone	28.3 ± 10.3	<0.1	12.11	6.34 ± 0.40
Metoprolol	15 ± 3	10 ± 3	4.28	4.51 ± 0.18
Timolol	7.7 ± 1.2	8 ± 4	2.09	0.92 ± 0.04
Sildenafil	6.0 ± 1.1	0	0.67	1.41 ± 0.08
Antipyrine	0.6 ± 0.2	2.8 ± 2.2	0.27	0.56 ± 0.06
Carbamazepine	0.36 ± 0.07	<1	0	0.07 ± 0.01